molbank

MDPI

Communication

Thorium(IV) and Uranium(IV) Complexes with 2,6-Dipicolinoylbis(*N*,*N*-diethylthiourea) Ligands

Christelle Njiki Noufele [1], Juliane März [2] and Ulrich Abram [1,*]

[1] Institute of Chemistry and Biochemistry, Freie Universität Berlin, Fabeckstr. 34/36, D-14195 Berlin, Germany; chrisnjiki@gmail.com
[2] Institute of Resource Ecology, Helmholtz-Zentrum Dresden-Rossendorf (HZDR), Bautzner Landstr. 400, D-01328 Dresden, Germany; j.maerz@hzdr.de
* Correspondence: ulrich.abram@fu-berlin.de

Abstract: The reaction of thorium nitrate hydrate with 2,6-dipicolinoylbis (*N*,*N*-diethylthiourea), H_2L^{pic}, results in the hydrolysis of the organic ligand and the formation of $[Th(2,6\text{-dipicolinolate})_2(H_2O)_4]$ (**1**). Hydrolysis can be avoided by the use of $[ThCl_4(DME)_2]$ (DME = 1,2-dimethoxyethane) as the starting material and the exclusion of water. The product, $[Th(L^{pic})_3]^{2-}$ (**2**), crystallizes as diammonium salt in form of yellow crystals in moderate yields. The thorium ion in the complex is nine-coordinate by the central *O*,*N*,*O* donor atoms of three deprotonated $\{L^{pic}\}^{2-}$ ligands. The sulfur atoms of the ligands do not bind to the actinide ion, but establish hydrogen bonds to the ammonium counter ions. A similar coordination sphere is also observed in the uranium(IV) complex $[UAu_2(L^{pic})_3\}]$ (**3**), which was obtained from a reaction between H_2L^{pic}, $[U_2I_6(1,4\text{-dioxane})_3]$ and [AuCl(tht)] (tht = tetrahydrothiophene) in the presence of triethylamine. Charge compensation is established by the linear coordination of two Au^+ ions between each two sulfur atoms of the ligands. The products have been studied by X-ray diffraction and IR spectroscopy. The actinide ions in both $\{L^{pic}\}^{2-}$ complexes have coordination number nine, but establish slightly different coordination spheres.

Keywords: thorium; uranium; gold; actinides; aroylthioureas

check for updates

Academic Editor: Nicholas Leadbeater

Received: 18 December 2024
Revised: 17 January 2025
Accepted: 20 January 2025
Published: 22 January 2025

Citation: Noufele, C.N.; März, J.; Abram, U. Thorium(IV) and Uranium(IV) Complexes with 2,6-Dipicolinoylbis(*N*,*N*-diethylthiourea) Ligands. *Molbank* **2025**, *2025*, 0. https://doi.org/

1. Introduction

2,6-Dipicolinoylbis(*N*,*N*-diethylthiourea), H_2L^{pic}, is a representative of the large class of aroylthiourea ligands, which was introduced into coordination chemistry research by Lothar Beyer et al. about 50 years ago with the first *S*,*O* chelates [1]. Since then, a huge number of complexes with main-group and transition metal ions have been synthesized and structurally characterized, including several hundreds of X-ray structures [2–4]. Most of them involve *S*,*O* chelates with ligands of the type HL^1 (see Figure 1). The development of aroylthiourea derivatives with more than one *S*,*O* chelating group and the introduction of additional donor atoms in a central aryl ring (e.g., compound H_2L^2, H_2L^{fur} or H_2L^{pic}) provide completely new synthetic opportunities, such as the access to complexes with "hard" donor atoms and the synthesis of multinuclear assemblies [5–11]. The synthesis of the latter compounds is supported by the central molecular position, which provides a coordinating *O*,*N*,*O* or *O*,*O*,*O* unit and is perfectly suitable for "medium" or "hard" metal ions, while the peripheral *O*,*S* donors prefer "soft" metal ions.

The selective choice of "hard" or "soft" donor atom positions for "hard" or "soft" metal ions aligns with the classical concept of Pearson [12]. This principle allows for the synthesis of complexes with "hard" lanthanide ions [13–17] and, more recently, the first uranyl complexes have also been isolated following this concept [18–20]. In the present paper, we present the first attempts to synthesize complexes of 2,6-dipicolinoylbis(*N*,*N*-diethylthiourea) with lower-valent actinide ions.

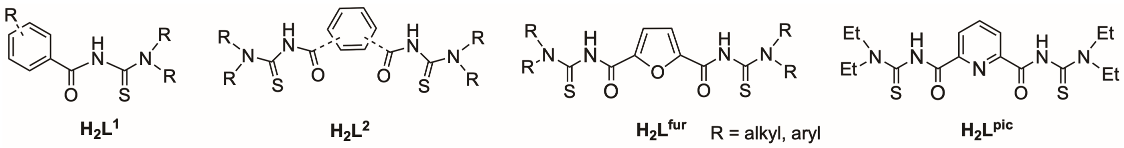

Figure 1. Aroylthioureas as potential chelating ligands.

2. Results and Discussion

The attempted reactions of $Th(NO_3)_4 \cdot 4\ H_2O$ with the proligand H_2L^{pic} in methanol or other alcohols did not result in the formation of thorium complexes with intact $\{L^{pic}\}^{2-}$ ligands. Instead, hydrolysis of the aroylthiourea units and the formation of 2,6-dipicolinate was observed, which finally reacted with the Th^{4+} ions under the formation of the complex $[Th(2,6\text{-dipicolinate})_2(H_2O)_4]$ (**1**); see Scheme 1. The compound precipitated from the reaction mixture as a colorless solid. Single crystals suitable for X-ray diffraction were obtained from CH_2Cl_2/MeOH.

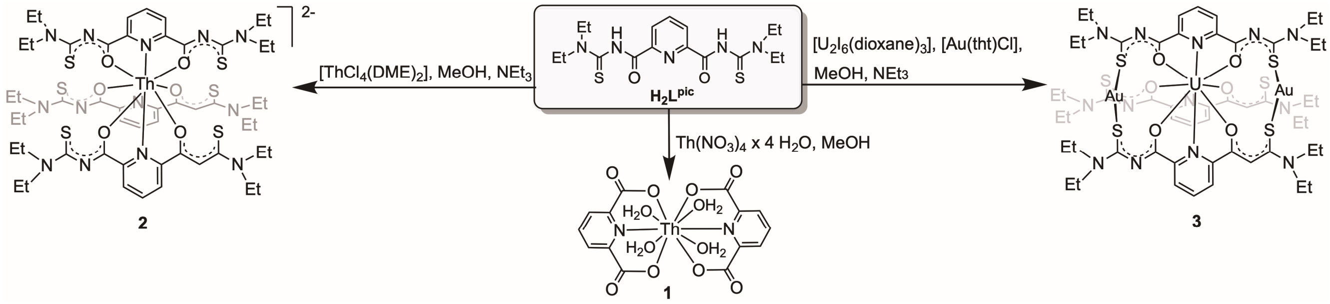

Scheme 1. The reactions of H_2L^{pic} with thorium(IV) and uranium(III) compounds and their products.

The observed reaction and the formation of a complex with the hydrolysis product 2,6-dipicolinic acid is not without precedent in the chemistry of the aroylthiourea ligands under study. Similar reactions giving the hexameric complex $[UO_2(2,6\text{-dipicolinate})(H_2O)]_6$ were observed during the treatment of H_2L^{pic} with uranyl compounds such as acetate, nitrate, or $(NBu_4)_2[UO_2Cl_4]$ [18]. Another type of hydrolysis, the conversion of a thiourea moiety into a coordinated urea unit, was observed when an excess of NEt_3 was added as a supporting base [20] to such mixtures, while the hydrolysis could be avoided with the addition of only a small amount of the supporting base [19]. The latter approach and the use of a non-aqueous thorium starting material and absolutely dry solvents also avoided the hydrolysis of H_2L^{pic} in reactions with thorium(IV) ions. Thus, the reaction of $[ThCl_4(DME)_2]$ (DME = 1,2-dimethoxyethane) with H_2L^{pic} in dry methanol gave the anionic tris chelate $[Th(L^{pic})_3]^{2-}$ (**2**). Yellow-brown single crystals of the product could be isolated as the diammonium salt after the addition of $(NH_4)PF_6$.

Compound **1** has been synthesized before by the treatment of $Th(NO_3)_4 \cdot 5\ H_2O$ with dipicolinic acid [21]. Since in this early work no details about the structure have been reported and no coordinates have been deposited in the Cambridge structural database, we decided to include some structural details of $[Th(2,6\text{-dipicolinate})_2(H_2O)_4]$ in the present communication. The compound crystallizes as hydrate in the monoclinic space group C2/c with two different molecules in the unit cell. One of these molecules contains the thorium atom Th2 located on a 2-fold symmetry axis, while the other molecule contains all atoms on general positions. The inherent symmetry in one of the complex molecules results in slight differences in the coordination spheres of the two thorium atoms. Ellipsoid representations of both individuals are shown in Figure 2, together with a visualization of the resulting coordination polyhedra. Some selected bond lengths are summarized in Table 1. Full listings of the bond lengths and angles are given as Supplementary Materials.

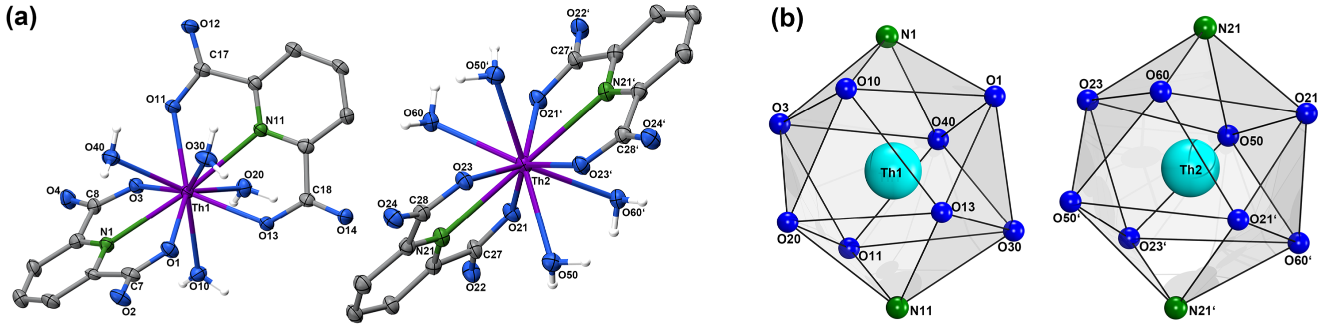

Figure 2. (**a**) A representation of the two independent species of [Th(2,6-dipicolinate)$_2$(H$_2$O)$_4$] in **1**. Thermal ellipsoids represent 30% probability. (**b**) Coordination polyhedra around the 10-coordinate thorium ions. For the color code, see the atomic labeling scheme. Symmetry code: (′) 1-x, y, 1.5-z.

Table 1. Selected bond lengths (Å) in [Th(2,6-dipicolinate)$_2$(H$_2$O)$_4$].

Th1–O1	2.427(4)	Th1–N1	2.629(5)	Th1–O3	2.432(4)	Th1–O11	2.411(4)	Th1–N11	2.620(5)
Th1–O13	2.437(4)	Th1–O10	2.551(4)	Th1–O20	2.583(5)	Th1–O30	2.581(4)	Th1–O40	2.503(5)
O1–C7	1.270(7)	C7–O2	1.242(7)	O3–C8	1.295(7)	C8–O4	1.236(7)	O11–C17	1.290(7)
C17–O12	1.228(6)	O13–C18	1.297(7)	C18–O14	1.234(7)	Th2–O21	2.419(4)	Th2–N21	2.629(5)
Th2–O23	2.417(4)	Th2–O50	2.544(4)	Th2–O60	2.583(4)	O21–C27	1.288(7)	C27–O22	1.234(7)
O23–C28	1.277(7)	C28–O24	1.238(7)						

The coordination polyhedra around both thorium atoms can be interpreted as a mixture between distorted bicapped square antiprisms and sphenocoronas, which corresponds to the situation in numerous complexes of coordination number ten [22]. A closer inspection with the SHAPE algorithm [23–28], however, shows that the polyhedron around thorium atom Th1 is better described as a sphenocorona, and that around Th2 is dominated by contributions of a bicapped square antiprism. A table containing the continuous SHAPE measures for all contributing polyhedra is given as Supplementary Materials.

The discussed differences are also found for the angles between the planes formed by the two planar chelating ligands binding to Th1 (47.6°) and Th2 (44.3°). No significant differences could be detected for the Th–N bond lengths, which are between 2.620(5) and 2.629(5) Å in both species, or for the Th–O$_{(carboxyl)}$ bonds (2.411(4) − 2.437(4) Å). The Th–O$_{(water)}$ bond lengths are variable in both species.

The chelate rings in compound **1** are exclusively formed by "hard" *O*,*N*,*O* donor atoms. A similar situation is obtained in the anion of compound **2**, which contains three intact $\{L^{pic}\}^{2-}$ ligands. The six sulfur atoms remain uncoordinated, but establish hydrogen bonds with the two ammonium counter ions. Details about the obtained H bond network are given as Supplementary Materials. The bonding situation in the $[Th(L^{pic})_3]^{2-}$ anion is illustrated in Figure 3a, and selected bond lengths are contained in Table 2. The deprotonation of aroylthioureas and related ligands in their transition metal complexes is common for corresponding *S*,*O* chelates [1–3,5–11], but has recently also been observed for other coordination modes, including a few complexes with the actinides uranium and thorium [17–20,28]. Such a bonding feature supports the formation of chelate rings with extended π-systems. Also, in the present case, the double deprotonation of H_2L^{pic} is observed, which causes marked changes in the bond lengths within the skeletons of the ligands with respect to the situation in the uncoordinated proligand [11]. Also, remarkably, peripheral bonds, such as the C–S bonds which are not directly concerned by the complex formation, are lengthened, while the frequently observed C–N bond equalization in the *S*,*O* chelates [1–3,5–11] does not apply in $[Th(L^{pic})_3]^{2-}$.

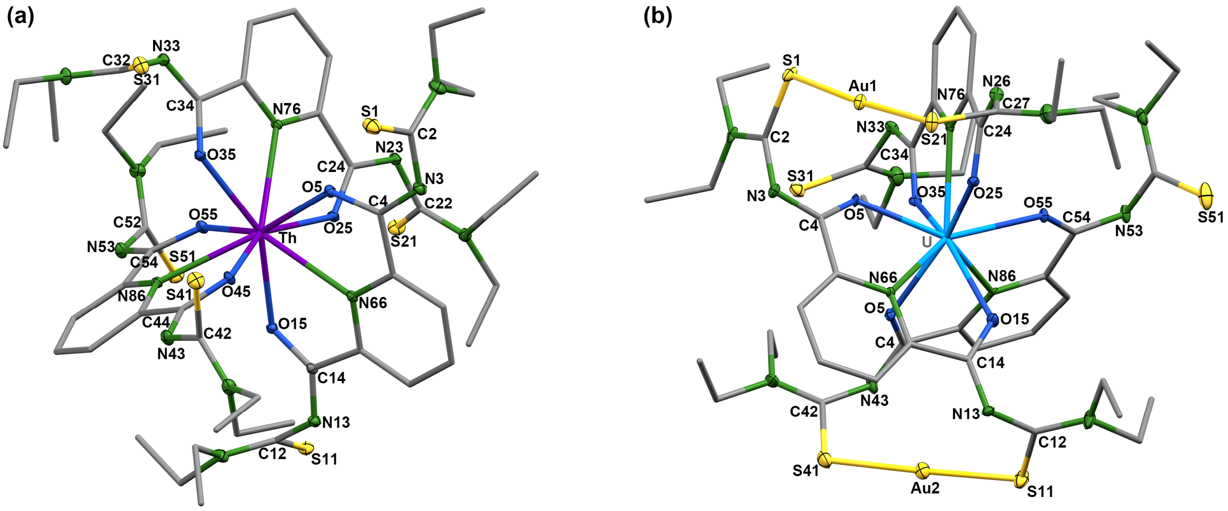

Figure 3. (**a**) A representation of the structures of the $[Th(L^{pic})_3]^{2-}$ anion of compound **2** and (**b**) of $[UAu_2(L^{pic})_3]$ (**3**). Thermal ellipsoids represent 30% probability. For the color code, see the atomic labeling scheme.

Table 2. Selected bond lengths (Å) in the $[Th(L^{pic})_3]^{2-}$ anion of **2** and (**b**) of $[UAu_2(L^{pic})_3]$ (**3**).

Compound 2									
Th–O5	2.426(1)	Th–O15	2.4266(9)	Th–N66	2.616(1)	Th–O25	2.4026(9)	Th1–O35	2.4321(9)
Th–N76	2.596(1)	Th–O45	2.4069(9)	Th–O55	2.4182(10)	Th–N86	2.598(1)	O5–C4	1.298(2)
C4–N3	1.293(2)	N3–C2	1.391(2)	C2–S1	1.691(2)	O15–C14	1.303(2)	C14–N13	1.293(2)
N13–C12	1.390(2)	C12–S11	1.706(2)	O25–C24	1.299(2)	C24–N23	1.290(2)	N23–C22	1.389(2)
C22–S21	1.693(1)	O35–C34	1.300(2)	C34–N33	1.289(2)	N33–C32	1.386(2)	C32–S31	1.693(1)
O45–C44	1.299(2)	C44–N43	1.286(2)	N43–C42	1.286(2)	C42–S41	1.7080(2)	O55–C54	1.298(2)
C54–N53	1.292(2)	N53–C52	1.392(2)	C52–S51	1.711(2)				
Compound 3									
U–O5	2.336(5)	U–O15	2.381(5)	U–N66	2.576(6)	U–O25	2.414(5)	U–O35	2.348(5)
U–N76	2.542(6)	U–O45	2.374(5)	U–O55	2.333(5)	U–N86	2.551(6)	O5–C4	1.286(9)
C4–N3	1.30(1)	N3–C2	1.35(1)	C2–S1	1.729(9)	O15–C14	1.282(9)	C14–N13	1.29(1)
N13–C12	1.37(1)	C12–S11	1.734(9)	O25–C24	1.285(9)	C24–N23	1.30(1)	N23–C22	1.35(1)
C22–S21	1.731(8)	O35–C34	1.294(9)	C34–N33	1.29(1)	N33–C32	1.39(1)	C32–S31	1.676(9)
O45–C44	1.295(9)	C44–N43	1.30(1)	N43–C42	1.37(1)	C42–S41	1.736(9)	O55–C54	1.294(9)
C54–N53	1.29(1)	N53–C52	1.29(1)	C52–S51	1.67(1)	Au1–S1	2.285(2)	Au1–S21	2.293(2)
Au2–S11	2.283(2)	Au2–S41	2.281(2)						

A similar bonding situation, with an actinide ion being coordinated by three $\{L^{pic}\}^{2-}$ ligands, is observed in $[UAu_2(L^{pic})_3]$ (**3**). This compound is formed during reactions of $[U_2I_6(1,4\text{-dioxane})_3]$ with H_2L^{pic} in the presence of [AuCl(tht)] (tht = tetrahythiophene) in dry THF. Although the reaction was carried out under anaerobic conditions in a glove box, the oxidation of the uranium(III) starting material was observed and a uranium(IV) complex was formed. This is not completely unexpected with respect to the redox potentials of the involved redox couples (U(III)/U(IV): −0.63 V and Au(I)/Au(0): +1.68 V).

The coordination environment of the uranium atom in compound **3** is similar to that of the thorium atom in compound **2**. Generally, the respective U–O and U–N bonds in **3** are somewhat shorter than the respective bonds around the thorium atom in **2**, which is in accord with the different ionic radii of the two actinide ions [29]. However, some exceptions apply, which can most probably be attributed to the influence of the peripheral coordination of four of the six sulfur atoms to Au(I) ions (Figure 3b). The fixation of these sulfur atoms in almost linear S–Au–S bonds (angles of 175.38(9)° and 177.04(9)° are observed) produces steric restraints, which also take effect in the coordination sphere of the uranium ion, as can be seen by some changes in its coordination environment (vide infra). The C–S bonds to the coordinating sulfur atoms are clearly longer than those to the non-coordinating atoms S31 and S51. The Au–S bond lengths are between 2.28 and 2.29 Å, which is in the range observed for corresponding cage compounds with lanthanide ions [17].

The thorium and uranium atoms in **2** and **3** have the coordination number nine. In a detailed structural survey of nine-coordinate metal complexes, it has been outlined that most of the compounds with mono- or bidentate ligands, as well as those with three tridentate grasping ligands, can be correlated with tricapped trigonal prismatic (TCTPR) or capped trigonal antiprismatic (CSAPR) coordination polyhedra [30]. This general information also holds true for the compounds of the present study, but neither compound **2** nor compound **3** are adequately described by only one of these ideal polyhedral, as becomes evident during a closer inspection by means of the SHAPE algorithm [23–27]. Also, the contributions of a tridiminished icosahedron (JTDIC) and a muffin (MFF) play a role. Figure 4 illustrates the coordination polyhedra of **2** (green) and **3** (blue). Additionally, the shape of contributing polyhedra together with their continuous SHAPE measures (CShM) are shown. The CShMs are read in such a way that the lower their numerical value, the higher the contribution of the idealized polyhedron to the geometry of the compound under study. Consequently, the coordination sphere of $[Th(L^{pic})_3]^{2-}$ (**2**) is best described by a spherical tricapped trigonal prism, while for $[UAu_2(L^{pic})_3]$ (**3**), a mixture of a spherical capped square antiprism, a tricapped trigonal prism, and a muffin is more suitable. More details and the values for the less relevant polyhedra are provided as Supplementary Materials.

We were able to demonstrate that the pyridine-centered aroylthiourea derivative H_2L^{pic} forms stable complexes with Th^{4+} and U^{4+} ions. In both cases, the central *O,N,O* donor atoms are exclusively used for the coordination of the actinides. The peripheral “soft” sulfur atoms can establish bonds to additional “soft” metal ions such as Au^+, as has been demonstrated for the uranium compound.

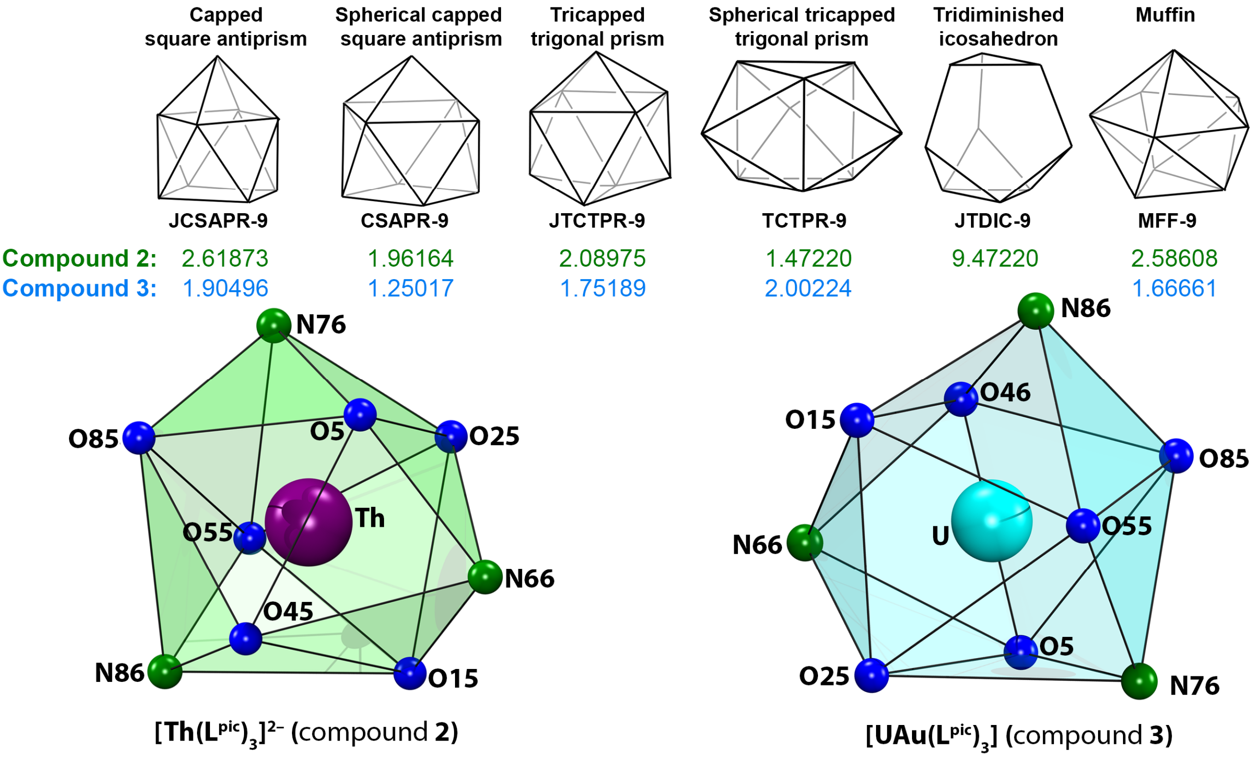

Figure 4. A representation of the coordination polyhedra of the Th^{4+} and U^{4+} ions in $[Th(L^{pic})_3]^{2-}$ (**2**) and $[UAu_2(L^{pic})_3]$ (**3**), together with idealized polyhedra, with significant contributions to their coordination spheres. The numbers represent the continuous SHAPE measures [23–27] of the respective polyhedra. The atomic labeling schemes and the color code correspond to the values used in Figure 3.

3. Materials and Methods

3.1. General Considerations

IR spectra were measured as KBr pellets on Shimadzu IR Affinity-1 (Shimadzu, Kyoto, Japan) or Agilent Cary 630 spectrometers (Agilent, Santa Clara, CA, USA). Elemental analyses of carbon, hydrogen, nitrogen, and sulfur were carried out using a Heraeus vario EL elemental analyzer (Elementar, Langensebold, Germany). The intensities for the X-ray determinations were collected on STOE IPDS T2 (STOE, Darmstadt, Germany) or Bruker D8 Venture (BRUKER, Billerica, MA, USA) instruments with Mo/Kα radiation. Absorption correction was carried out with the APEX 3 software (version 1.0) suite and the STOE XRED32 routine [31,32]. Structure solution and refinement were performed with the SHELX programs [33,34] included in OLEX2, version 1.5 [35]. Hydrogen atoms were calculated for idealized positions and treated with the 'riding model' option of SHELXL. Details are given as Supplementary Materials. The representation of the molecular structures was achieved using the program MERCURY, version 2024, 2.0 [36].

3.2. Radiation Precautions

All synthetic work with thorium or uranium compounds was performed in a laboratory approved for the handling of radioactive material. All personnel working on this project were permanently monitored for potential contaminations.

3.3. Synthesis of $[Th(2,6\text{-dipicolinate})_2(H_2O)_4]$ (**1**)

H_2L^{Pic} (39.5 mg, 0.1 mmol) was dissolved in MeOH (3 mL) and added to a solution of $Th(NO_3)_2 \cdot 4\ H_2O$ (50.2 mg, 0.1 mmol) in MeOH (3 mL). The reaction mixture was stirred at room temperature for 1 h. The obtained colorless precipitate was filtered off, washed with MeOH, and dried under vacuum. Single crystals for X-ray diffraction were obtained by a slow evaporation of a CH_2Cl_2/MeOH 1:1 (v/v) solution at room temperature. Yield: 30% (19 mg). Elemental analysis: calculated for $C_{14}H_{14}N_2O_{12}Th$: C, 26.5; H, 2.2; N, 4.4%. Found: C, 25.9; H, 2.4; N, 4.3%. IR (KBr, cm^{-1}): 3449(s), 3094(w), 3046(m), 2926(w), 1626(vs), 1427(s), 1377(vs), 1271(m), 1186(m), 1078 (s), 1018(m), 921(m), 860(m), 773(s), 729(s), 691(s), 586 (m), 520(w), 411(m).

3.4. Synthesis of $(NH_4)_2[Th(L^{pic})_3]$ (**2**)

The reaction was performed in an MBraun MB 200B glove box under an argon atmosphere. H_2L^{pic} (39.5 mg, 0.1 mmol) was added to a stirred solution of $[ThCl_4(DME)_2]$ (20.3 mg, 0.05 mmol) in dry MeOH (3 mL). After 20 min, 3 drops of NEt_3 were added and the reaction mixture was stirred at room temperature for 1 h. $NH_4(PF_6)$ (16 mg, 0.1 mmol) was added to the reaction mixture. The color of the solution turned to yellow-green. After 1 h, the mixture was filtered and overlayered with diethyl ether. Single crystals for X-ray diffraction were obtained by slow diffusion of the solvents. Yield: 60% (44.7 mg). IR (KBr, cm^{-1}): 2974(m), 2932(m), 2603(m), 2496(m), 1590(s), 1566(s), 1493(s), 1481(s), 1420(m), 1366(vs), 1306(m), 1278(m), 1243(s), 1203(w), 1172(w), 1158(w), 1121(m), 1097(m), 1065(s), 1035(m), 1019(m), 948(m), 912(s), 876(s), 836(vs), 763(s), 700(m), 683(w), 658(w). Elemental analysis could not be determined for the air- and moisture-sensitive products due to radiation protection restrictions.

3.5. Synthesis of $[UAu_2(L^{pic})_3]$ (**3**)

The reaction was performed in an MBraun MB 200B glove box under an argon atmosphere. H_2L^{pic}) 39.5 mg, 0.1 mmol) and [Au(tht)Cl] (32 mg, 0.1 mmol) were added to a stirred solution of $[U_2I_6(1,4\text{-dioxane})_3]$ (75.2 mg, 0.05 mmol) in THF (3 mL). After 20 min, 3 drops of NEt_3 were added and the reaction mixture was stirred for another 1 h. The color of the solution turned brown, and a dark, insoluble precipitate was formed. The solid was filtered off and washed with THF. Filtrates were collected and overlayered with diethyl ether. Single crystals for X-ray diffraction were obtained by slow diffusion of the solvents. Yield: 40% (36 mg). Elemental analysis: calculated for $C_{51}H_{69}N_{15}O_6S_6U\cdot(C_4H_8O)$: C, 35.0; H, 4.1; N, 11.2; S, 10.2%. Found: C, 35.0; H, 4.2; N, 11.2; S, 10.2%. IR (KBr, cm^{-1}): 2971(s), 2931(s), 2872(w), 2764(m), 2681(m), 2479(w), 1577(s), 1559(vs), 1523(vs) 1420(s), 1390(s), 1309(m), 1290(m), 1238(s), 1197(m), 1146(m), 1117(m), 1067(m), 1018(m), 947(m), 910(s), 870(m), 835(m), 794(m), 770(s), 752(m), 730(m), 695(m).

Supplementary Materials: The following supporting information can be downloaded at: https://www.mdpi.com/article/10.3390/0/s1, Table S1: Crystallographic data and data collection parameters. Figure S1: An ellipsoid representation of the structure of 3 $[Th(2,6\text{-dipicolinolate})_2(H_2O)_4]\cdot 4\ H_2O$. The thermal ellipsoids are set at a 30% probability level. Hydrogen atoms bonded to carbon atoms are omitted for clarity. Table S2: Bond lengths (Å) in 3 $[Th(2,6\text{-dipicolinolate})_2(H_2O)_4]\cdot 4\ H_2O$. Table S3: Bond angles (°) in 3 $[Th(2,6\text{-dipicolinolate})_2(H_2O)_4]\cdot 4\ H_2O$. Figure S2: An ellipsoid representation of the structure of $(NH_4)_2[Th(L^{pic})_3]\cdot$MeOH, also illustrating the positional disorders of some sulfur atoms. The thermal ellipsoids are set at a 30% probability level. Hydrogen atoms bonded to carbon atoms are omitted for clarity. Table S4: Bond lengths (Å) in $(NH_4)_2[Th(L^{pic})_3]\cdot$MeOH. Table S5: Bond angles (°) in $(NH_4)_2[Th(L^{pic})_3]\cdot$MeOH. Figure S3: The hydrogen bonding network between the complex anion and the two ammonium cations in $(NH_4)_2[Th(L^{pic})_3]\cdot$MeOH. Figure S4: An ellipsoid representation of the structure of $[UAu_2(L^{pic})_3]\cdot$THF, also illustrating the positional disorders of two ethyl groups. The thermal ellipsoids are set at a 30% probability level. Hydrogen atoms bonded to carbon atoms are omitted for clarity. Table S6: Bond lengths (Å) in $[UAu_2(L^{pic})_3]\cdot$THF. Table S7: Bond angles (°) in $[UAu_2(L^{pic})_3]\cdot$THF. Figure S5: IR spectrum (KBr) of $[Th(2,6\text{-dipicolinolate})_2(H_2O)_4]$. Figure S6: IR spectrum of $(NH_4)_2[Th(L^{pic})_3]$. Figure S7: IR spectrum of [$UAu_2(L^{pic})_3$]. Table S8: The continuous SHAPE measures (CShM) for the ten-coordinate complex [Th(2,6-dipicolinolate)$_2$(H_2O)$_4$], considering all idealized relevant polyhedra. Polyhedra with significant distributions are highlighted. Table S9: The continuous SHAPE measures (CShM) for the nine-coordinate complexes (NH_4)$_2$[Th(L^{pic})$_3$] and [$UAu_2(L^{pic})_3$], considering all idealized relevant polyhedra. Polyhedra with significant distributions are highlighted.

Author Contributions: Conceptualization, C.N.N. and U.A.; methodology, C.N.N. and J.M.; validation, C.N.N., J.M. and U.A.; formal analysis, C.N.N. and J.M.; investigation, C.N.N., J.M. and U.A.; resources, U.A.; data curation, C.N.N. and U.A.; writing—original draft preparation, U.A.; writing—review and editing, C.N.N., J.M. and U.A; visualization, U.A.; supervision, U.A.; project administration, U.A.; funding acquisition, C.N.N. and U.A. All authors have read and agreed to the published version of the manuscript.

Funding: This research was funded by the Rosa Luxemburg Foundation (PhD scholarship to C.N.N.).

Data Availability Statement: Data are contained within the article and the Supplementary Materials.

Acknowledgments: We would like to acknowledge the assistance of the Core Facility BioSupraMol supported by the DFG.

Conflicts of Interest: The authors declare no conflicts of interest.

References

1. Beyer, L.; Hoyer, E.; Hennig, H.; Kirmse, R.; Hartmann, H.; Liebscher, J. Synthese und Charakterisierung neuartiger Übergangsmetallchelate von 1,1-Dialkyl-3-benzoyl-thioharnstoffen. *J. Prakt. Chem.* **1975**, *317*, 829–839. [CrossRef]
2. Beyer, L.; Hoyer, E.; Liebscher, J.; Hartmann, H. Komplexbildung mit N-Acyl-thioharnstoffen. *Z. Chem.* **1981**, *21*, 81–91. [CrossRef]
3. Koch, K.R. New chemistry with old ligands: N-alkyl- and N, N-dialkyl-N′-acyl(aroyl)thioureas in co-ordination, analytical and process chemistry of the platinum group metals. *Coord. Chem. Rev.* **2001**, *216−217*, 473–488. [CrossRef]
4. Cambridge Crystallographic Database, Version 5.44. Available online: https://www.ccdc.cam.ac.uk (accessed on 1 December 2024).
5. Koch, K.R.; Bourne, S.A.; Coetzee, A.; Miller, J. Self-assembly of 2:2 and 3:3 metallamacrocyclic complexes of platinum(II) with symmetrical, bipodal *N*′,*N*′,*N*‴,*N*‴-tetraalkyl-*N*,*N*″-phenylenedicarbonylbis(thiourea). *J. Chem. Soc. Dalton Trans.* **1999**, 3157–3161. [CrossRef]
6. Rodenstein, A.; Griebel, J.; Richter, R.; Kirmse, R. Synthese, Struktur und EPR-Untersuchungen von binuklearen Bis(*N*,*N*,*N*‴,*N*‴-tetraisobutyl-*N*′,*N*″-isophthaloylbis(thioureato))-Komplexen des Cu^{II}, Ni^{II}, Zn^{II}, Cd^{II} und Pd^{II}. *Z. Anorg. Allg. Chem.* **2008**, *634*, 867–874. [CrossRef]
7. Koch, R.K.; Hallale, O.; Bourne, S.A.; Miller, J.; Bacsa, J. Self-assembly of 2:2 metallomacrocyclic complexes of Ni^{II} and Pd^{II} with 3,3,3′,3′-tetraalkyl-1,1′-isophthaloylbis(thioureas). Crystal and molecular structures of *cis*-[Pd(L^2-*S*,*O*)]$_2$ and the adducts of the corresponding Ni^{II} complexes: [Ni(L^1-*S*,*O*)(pyridine)$_2$]$_2$ and [Ni(L^1-*S*,*O*)(4-dimethylaminopyridine)$_2$]$_2$. *J. Mol. Struct.* **2001**, *561*, 185–196.
8. Westra, A.N.; Bourne, S.A.; Koch, K.R. First metallamacrocyclic complexes of Pt(iv) with 3,3,3′,3′-tetraalkyl-1,1′-phenylenedicarbonylbis(thioureas): Synthesis by direct or electrolytic oxidative addition of I_2, Br_2 and Cl_2. *Dalton Trans.* **2005**, 2916–2924. [CrossRef] [PubMed]
9. Keskin, E.; Solmaz, U.; Gumus, I.; Arslan, H. Di- and tetra-nuclear oxorhenium(V) complexes of benzoylthiourea derivative ligands: Synthesis, structural characterization, and catalytic applications. *Polyhedron* **2022**, *219*, 115786. [CrossRef]
10. Teixeira, E.I.; Schwalm, C.S.; Casagrande, G.A.; Tirloni, B.; Schwade, V.D. Binuclear isophthaloyl*bis*(*N*,*N*-diphenylthioureate) transition metal complexes: Synthesis, spectroscopic, thermal and structural characterization. *J. Mol. Struct.* **2020**, *1210*, 127999. [CrossRef]
11. Pham, C.T.; Roca Jungfer, M.; Abram, U. Indium(III) {2}-Metallacryptates Assembled from 2,6-Dipicolinoyl-bis(*N*,*N*-diethylthiourea. *New J. Chem.* **2020**, *44*, 3672–3680. [CrossRef]
12. Pearson, R.G. Hard and Soft Acids and Bases. *J. Am. Chem. Soc.* **1963**, *85*, 3533–3539. [CrossRef]
13. Pham, C.T.; Nguyen, T.H.; Trieu, T.N.; Matsumoto, K.; Nguyen, H.H. Syntheses, Structures, and Magnetism of Trinuclear Zn_2*Ln* Complexes with 2,6-Dipicolinoylbis(*N*,*N*-diethylthiourea). *Z. Anorg. Allg. Chem.* **2019**, *645*, 1072–1078. [CrossRef]
14. Jesudas, J.J.; Pham, C.T.; Hagenbach, A.; Abram, U.; Nguyen, H.H. Trinuclear ‘$Co^{II}Ln^{III}Co^{II}$’ Complexes (Ln = La, Ce, Nd, Sm, Gd, Dy, Er and Yb) with 2,6-Dipicolinoyl-bis(*N*,*N*-diethylthiourea)—Synthesis, Structures and Magnetism. *Inorg. Chem.* **2020**, *58*, 386–395. [CrossRef] [PubMed]

15. Pham, C.T.; Nguyen, T.H.; Matsumoto, K.; Nguyen, H.H. Cu^I/Cu^{II} Complexes with Dipicolinoylbis(*N*,*N*-diethylthiourea): Structures, Magnetism, and Guest Ion Exchange. *Eur. J. Inorg. Chem.* **2019**, *2019*, 4142–4146. [CrossRef]
16. Le, C.D.; Pham, C.T.; Nuyen, H.H. Zinc(II) {2}-Metallacoronates and {2}-Metallacryptates based on Dipicolinoylbis(*N*,*N*-diethylthiourea): Structures and Biological Activities. *Polyhedron* **2019**, *173*, 114143. [CrossRef]
17. Sucena, S.F.; Demirer, T.I.; Baitullina, A.; Hagenbach, A.; Grewe, J.; Spreckelmeyer, S.; März, J.; Barkleit, A.; daSilva Maia, P.I.; Nguyen, H.H.; et al. Gold-based Coronands as Hosts for M^{3+} Metal Ions: Ring Size Matters. *Molecules* **2023**, *28*, 5421. [CrossRef] [PubMed]
18. Noufele, C.N.; Hagenbach, A.; Abram, U. Uranyl Complexes with Aroylbis(*N*,*N*-dialkylthioureas). *Inorg. Chem.* **2018**, *57*, 12255–12269. [CrossRef] [PubMed]
19. Noufele, C.N.; Schulze, D.; Roca Jungfer, M.; Hagenbach, A.; Abram, U. Bimetallic Uranium Complexes with 2,6-Dipicolinoylbis(*N*,*N*-dialkylthioureas). *Molecules* **2024**, *29*, 5001. [CrossRef]
20. Noufele, C.N.; Roca Jungfer, M.; Nguyen, H.H.; Hagenbach, A.; Abram, U. Uranium-mediated Thiourea/Urea Conversion on Chelating Ligands. *Inorganics* **2024**, *12*, 295. [CrossRef]
21. Degretto, S.; Baracco, L.; Graziani, R.; Celon, E. Preparation and Characterization of some Pyridine-2,3-dicarboxylato Thorium(IV) Complexes. *Transition Met. Chem.* **1978**, *3*, 351–354. [CrossRef]
22. Ruiz-Martínez, A.; Alvarez, S. Stereochemistry of Compounds with Coordination Number Ten. *Chem. Eur. J.* **2009**, *15*, 7470–7480. [CrossRef] [PubMed]
23. Zabrodsky, H.; Peleg, S.; Avnir, D. Continuous Symmetry Measures. *J. Am. Chem. Soc.* **1992**, *114*, 7843–7851. [CrossRef]
24. Pinsky, M.; Avnir, D. Continuous Symmetry Measures. 5. The Classical Polyhedra. *Inorg. Chem.* **1998**, *37*, 5575–5582. [CrossRef] [PubMed]
25. Alvarez, S. Polyhedra in (inorganic) chemistry. *Dalton Trans.* **2005**, 2209–2233. [CrossRef]
26. Alvarez, S.; Alemany, P.; Casanova, D.; Cirera, J.; Llunell, M.; Avnir, D. Shape maps and polyhedral interconversion paths in transition metal chemistry. *Coord. Chem. Rev.* **2005**, *249*, 1693–1708. [CrossRef]
27. Llunell, M.; Casanova, D.; Cirera, J.; Alemany, P.; Alvarez, S. Shape—Program for the Stereochemical Analysis of Molecular Fragments by Means of Continuous Shape Measures and Associated Tools, Version 2.1. University of Barcelona. Available online: https://www.ee.ub.edu/downloads/ (accessed on 10 December 2024).
28. Noufele, C.N.; Pham, C.T.; Abram, U. Bis{μ-(2,2′-bipyridine-1κ2N,N′)-(6,6′-dicarbonyl-1κ2O,O′:2κO′)bis(N,N-diethylthioureato-2κS)}(acetato-1κO)(μ-acetato-1κO:2-κO′)(methanol-2κO)thoriumnickel. *Molbank* **2025**, *2025*, M1948. [CrossRef]
29. Shannon, R.D. Revised Effective Ionic Radii and Systematic Studies of Interatomic Distances in Halides and Chalcogenides. *Acta Cryst.* **1976**, *A32*, 751–767. [CrossRef]
30. Ruiz-Martinez, A.; Casanova, D.; Alvarez, S. Polyhedral Structures with an Odd Number of Vertices: Nine-Coordinate Metal Compounds. *Chem. Eur. J.* **2008**, *14*, 1292–1303. [CrossRef] [PubMed]
31. *APEX 3 Software Suite*, version 1.0; Bruker: Billerica, MA, USA, 2016.
32. Coppens, P. *The Evaluation of Absorption and Extinction in Single-Crystal Structure Analysis. Crystallographic Computing*; Muksgaard: Copenhagen, Denmark, 1979.
33. Sheldrick, G.M. A short history of SHELX. *Acta Crystallogr.* **2008**, *64*, 112–122. [CrossRef] [PubMed]
34. Sheldrick, G.M. Crystal structure refinement with SHELXL. *Acta Crystallogr.* **2015**, *71*, 3–8.
35. Dolomanov, O.V.; Bourhis, L.J.; Gildea, R.J.; Howard, J.A.; Puschmann, H. OLEX2: A complete structure solution, refinement and analysis program. *J. Appl. Crystallogr.* **2009**, *42*, 339–341. [CrossRef]
36. Macrae, C.F.; Sovago, I.; Cottrell, S.J.; Galek, P.T.A.; McCabe, P.; Pidcock, E.; Platings, M.; Shields, G.P.; Stevens, J.S.; Towler, M. Mercury 4.0: From visualization to analysis, design and prediction. *J. Appl. Cryst.* **2020**, *53*, 226–235. [CrossRef] [PubMed]